Journal of
Manufacturing and
Materials Processing

MDPI

Article

Dynamic Reuleaux Venturi with Boundary-Imposed Swirl

Lorenzo Albanese

Institute of Bioeconomy, National Research Council of Italy, Via Madonna del Piano 10, 50019 Florence, Italy; lorenzo.albanese@cnr.it

Abstract

In-line cavitation is relevant to many continuous processes; however, its intensity depends on flow rate, available pressure, temperature, fluid properties, and plant conditions, complicating the maintenance of a repeatable regime within a prescribed band. This paper presents the DVRA, an actuated Venturi module with a Reuleaux triangular cross-section for in-operation regulation of hydrodynamic cavitation through device configuration. The novelty lies in combining two degrees of freedom—an in-operation adjustable hydraulic throat and boundary-imposed swirl forcing—within a compact in-line device: all rotation is confined to the module, and no rotation of the process line is required. The hydraulic throat is tuned via an actuated elastomeric liner, while swirl is generated by external end collars. Reproducible operational conventions are introduced together with a normalized input set and a configuration-space formalism that distinguishes admissible from achievable configurations. Regulation is cast as a control-oriented inverse mapping given a target band for an in-line estimated cavitation indicator and standard industrial measurements of flow rate, pressure, and temperature; configuration commands are selected to keep the indicator within bounds. The contribution is methodological and provides an implementable basis; comprehensive validation and performance benchmarking are outside the scope of this paper and will be reported separately.

Keywords: Reuleaux-section Venturi; boundary-imposed swirl; actuatable throat; control-oriented framework; inverse mapping

1. Introduction

In industrial practice, in-line hydrodynamic cavitation is commonly generated by static devices designed for a specific operating point, including Venturi devices with a circular throat [1–6]. In real processes, however, the processed medium and operating conditions evolve over time due to variations in temperature, viscosity, and gas or solids content, while the device geometry remains unchanged [7–9]. As a result, maintaining an optimal cavitation regime within a prescribed process window becomes difficult over extended operating periods [7,8,10]. In this context, controlled hydrodynamic cavitation is often intended as the regulation of operating conditions using plant-measurable variables, without modifying the installed cavitation generator [10].

At the same time, many studies on cavitating Venturi devices focus on geometric design, optimization, and flow characterization, while assuming a configuration defined at the design stage and then kept constant during operation [11–16]. Variable-geometry Venturi devices have been developed in other fields to modulate performance quantities such as pressure drop or collection efficiency, but their objective differs from maintaining a cavitation regime within a target band for processing and treatment applications [17–21].

Academic Editor: Steven Y. Liang

Received: 30 January 2026
Revised: 17 February 2026
Accepted: 25 February 2026
Published: 26 February 2026

In the available literature, variable-geometry Venturi concepts are most often based on the actuation of a single geometric variable, with throat adjustment used to influence global performance measures. This approach is not usually presented within a normalized configuration-space framework aimed at control-oriented cavitation regulation, and it does not explicitly address the requirement of maintaining cavitation intensity within a prescribed band under time-varying process conditions. Furthermore, independently imposed swirl forcing is not commonly treated as a second actuated variable to be coordinated with throat reconfiguration. Finally, the distinction between configurations that are admissible by design and those that are physically achievable in operation is not always made explicit [17–21].

From a plant perspective, it therefore remains relevant to formalize a reconfigurable cavitating Venturi that preserves in-line integration by keeping external interfaces unchanged, while making the internal configuration an operating variable for stabilizing and positioning the cavitation regime with respect to a defined process target.

In many process-intensification and extraction scenarios, the optimal cavitation operating window for a given target compound is not known as a priori and cannot be inferred reliably from design-stage assumptions.

A reconfigurable Venturi can therefore be used as a scouting and characterization platform: the throat configuration and boundary conditions are intentionally swept within a declared admissible/achievable set to identify the configuration and operating conditions that maximize a process performance metric (e.g., extraction yield, selectivity, purity, or minimal degradation) under the actual fluid properties and plant constraints.

Once this target window is identified, the same module can be operated either as a fixed-configuration device (set-and-lock) for a single-compound production line, or as an in-line actuator for maintaining the target performance under feed and operating variability through configuration-based regulation.

This work proposes the DVRA, a Reuleaux-section Venturi module designed for in-operation regulation of the cavitation regime through device configuration [22–24]. The module integrates two configuration degrees of freedom. The first is a reconfigurable effective hydraulic throat implemented through an actuated elastomeric liner, with a clear distinction between a reference throat and the effective hydraulic throat [19–21]. The second is boundary-imposed swirl forcing achieved through rotational boundary conditions applied at the module ends by external collars, without rotating parts immersed in the fluid and without requiring rotation of the process line. Operational definitions and conventions are introduced to provide an unambiguous and reproducible description of the device configuration, and a configuration space is formalized using normalized inputs, distinguishing admissible configurations from those that are practically achievable. A control-oriented framework casts regulation as an inverse mapping based on an in-line cavitation indicator estimated from standard industrial measurements of flow rate, pressure, and temperature.

This manuscript focuses on device architecture, operational definitions, and the configuration-space framework, while application-specific characterization and performance assessment are addressed separately.

The remainder of the manuscript presents the device architecture, the operational definitions required for a reproducible configuration description, and the control-oriented formulation of the regulation problem.

2. Operational Definitions and Notation

To describe the DVRA in a clear, unambiguous, and reproducible manner, this section introduces operational definitions for the throat, the actuation inputs, and the rotational boundary conditions. No predictive models are introduced.

From a fluid-dynamics perspective, the device retains the structure of a Venturi and includes a converging section, a throat region, and a diverging section. To make the geometry and boundary conditions unambiguous, three reference sections are defined. Section A identifies the DVRA inlet, section B identifies the outlet, and section T identifies the reference section at the throat. This choice makes it possible to distinguish two functional segments, A-T and T-B, which are used to define upstream and downstream rotational forcing with respect to the throat.

In the DVRA, a distinction is required between the reference throat and the effective hydraulic throat. The reference throat is a geometric and structural reference used to describe the device. The effective hydraulic throat coincides with the internal surface actally seen by the fluid and is determined by the elastomeric liner; therefore, it is a configurational quantity and can vary during operation. The hydraulic throat can be described operationally through equivalent geometric quantities, including the throat area A_T, the wetted perimeter P_T, and the equivalent hydraulic diameter $d_{eq} = 4A_T/P_T$ [8].

Reconfiguration of the hydraulic throat is specified by normalized inputs $u_i(t) \in [0,1]$, with $i = 1, \ldots, N$. Boundary swirl forcing is specified by $u_A(t) \in [0,1]$ and $u_B(t) \in [0,1]$. The vector of dimensionless inputs is defined as

$$\mathbf{u}(t) = [u_1(t), \ldots, u_N(t),\ u_A(t), u_B(t)]^T \quad (1)$$

where $u_1(t), \ldots, u_N(t)$ specify liner reconfiguration and $u_A(t)$, $u_B(t)$ specify boundary-imposed swirl forcing. Throat geometric quantities, such as $A_T(\cdot)$, $P_T(\cdot)$, and the derived equivalent quantities, are treated as functions of the throat subvector $\mathbf{u}_g(t) = [u_1(t), \ldots, u_N(t)]^T$ and can be obtained through a geometric–kinematic mapping or calibration. Swirl forcing is imposed as a rotational boundary condition at the module ends and is described by the angular velocities $\omega_A(t)$ at the inlet (section A) and $\omega_B(t)$ at the outlet (section B). These angular velocities are applied through external wheels or collars. Rotation is transferred to the internal DVRA structure, including the mechanical cage and the elastomeric liner, and does not require rotation of the process line.

The essential device element consists of three rigid segments A-T-B connected by 360° spherical joints. Operation can occur in a locked state, in which no relative rotation is allowed between segments, or in a free state, in which relative rotations are allowed. This distinction provides an unambiguous description of whether a differential rotational forcing can be applied across the throat.

To separate upstream and downstream rotational forcing with respect to the throat section T, relative rotations are introduced for the two module segments. The relative rotation in the A-T segment is defined as

$$\Omega_{AT}(t) = \omega_A(t) - \omega_T(t) \quad (2)$$

where $\omega_T(t)$ is the angular velocity associated with the throat reference section T. Similarly, the relative rotation in the T-B segment is defined as

$$\Omega_{TB}(t) = \omega_T(t) - \omega_B(t) \quad (3)$$

The quantities $\Omega_{AT}(t)$ and $\Omega_{TB}(t)$ are introduced as operational conventions to distinguish and compare rotational forcing upstream and downstream of section T. These definitions provide the basis for the classification of the operating modes introduced in the following sections. The quantity $\omega_T(t)$ is a kinematic reference associated with section T. When the throat reference at T is locked, $\omega_T = 0$ in the external (non-rotating) frame; hence $\Omega_{AT} = \omega_A$ and $\Omega_{TB} = -\omega_B$. When the reference at T is free, ω_T is not imposed and can be treated as an internal variable. In that case, explicit evaluation of Ω_{AT} and Ω_{TB} requires measuring ω_T (e.g., an encoder at T) or estimating it from the A-T-B kinematics; mode selection can still be implemented operationally by enforcing the locked/free constraints and by the imposed boundary conditions at A and B.

3. DVRA Architecture and In-Line Integration

The DVRA is a Reuleaux-section Venturi module designed for in-line installation and for use as an actuatable component in continuous processes. The regulation function is integrated into the device through an architecture that combines a continuous internal surface, defined by an elastomeric liner, with a constraint-and-guidance structure consisting of a mechanical cage, which transfers the commands and imposes the kinematic envelope. A consistent color code is adopted throughout the manuscript to identify the subsystems, namely the reference throat (yellow), the structural cage (white), the elastomeric liner and hydraulic surface (red), the liner actuators (blue), and the 360° spherical joints (black). An overall view of the module is reported in Figure 1.

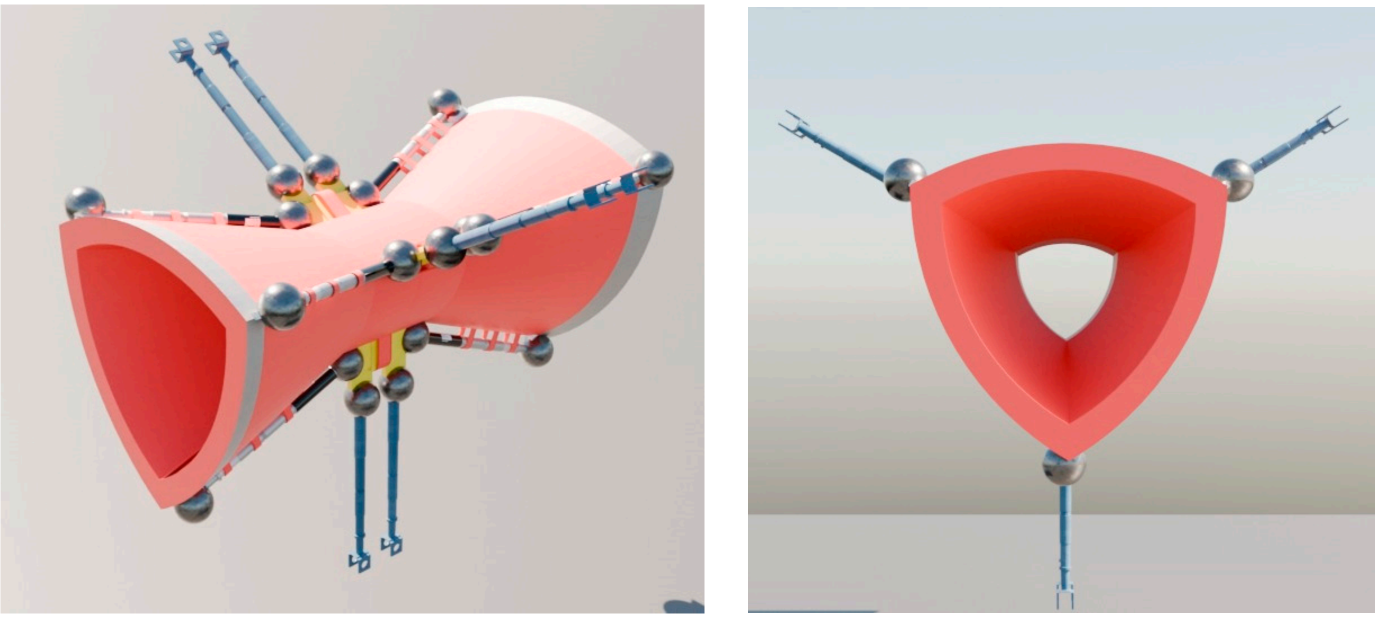

(a) (b)

Figure 1. DVRA module with Reuleaux cross-section in the baseline configuration. (**a**) Overall view highlighting the internal subsystem made of the mechanical cage and the elastomeric liner, the actuation system, and the 360° spherical joints. (**b**) Front view of the Reuleaux section highlighting the internal hydraulic surface defined by the elastomeric liner. Color code: reference throat (yellow), structural cage (white), elastomeric liner/hydraulic surface (red), liner actuators (blue), and 360° spherical joints (black).

From a fluid-dynamics perspective, the device retains the classical Venturi structure, including a converging section, a throat region, and a diverging section. From a mechanical perspective, the combination of the cage and the liner separates the structural reference from the effective hydraulic section. The reference throat provides a stable geometric frame, whereas the effective hydraulic section can be modified during operation through controlled liner deformation. The liner enables a continuous change in the cross-section without internal wall discontinuities (Figure 2). The cage guides the deformation and bounds its operating domain, thereby contributing to configuration repeatability.

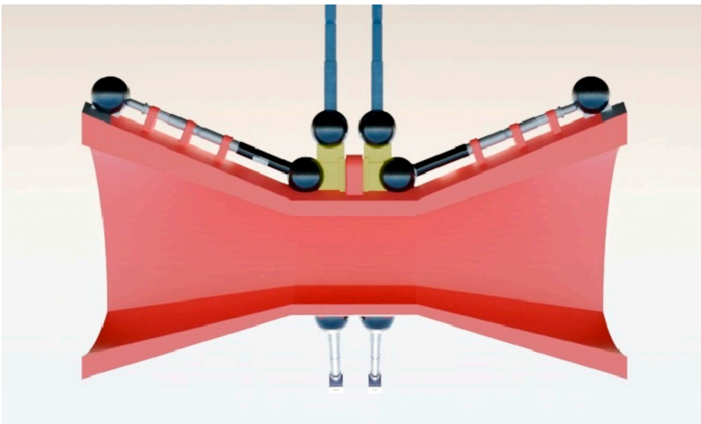

Figure 2. DVRA cross-sectional view. Color code: reference throat (yellow), structural cage (white), elastomeric liner/hydraulic surface (red), liner actuators (blue), and 360° spherical joints (black).

The essential construction unit of the DVRA is an element composed of three rigid segments A-T-B, connected by 360° spherical joints that allow relative rotations and local misalignments between components. This architecture reduces undesirable kinematic constraints when torsion and throat-surface deformation are combined. Operationally, the A-T-B element can operate in a locked state, in which relative rotations between segments are not allowed, or in a free state, in which relative rotations are allowed. The logic of the elementary module and the use of the spherical joints are illustrated in Figure 3.

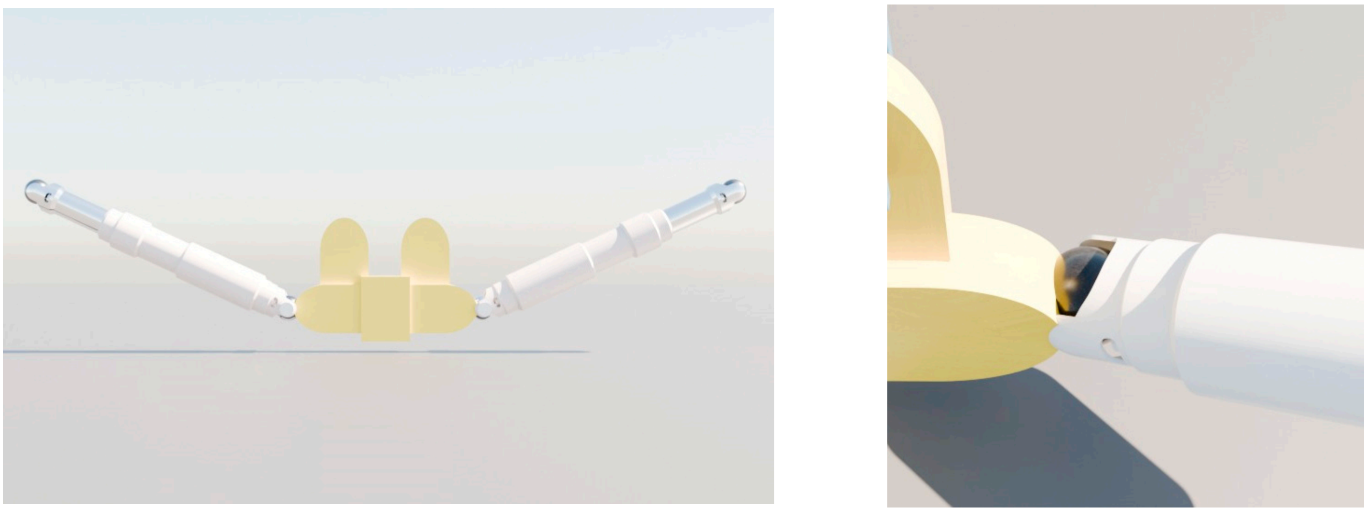

(**a**) (**b**)

Figure 3. Elementary module. (**a**) Overall view. (**b**) Detail of the 360° spherical joint. Color code: reference throat (yellow), structural cage (white), and 360° spherical joint (black).

For in-line integration of the DVRA, geometric transitions between circular pipes and the Reuleaux cross-section are provided to ensure compatibility with connections and constraints typical of continuous-process plants. When enabled, swirl forcing is implemented through external wheels or collars at ends A and B. Collar rotation imposes the angular velocities $\omega_A(t)$ and $\omega_B(t)$ and transfers motion to the internal DVRA structure. An overall view of the integration and the collar placement at the ends are reported in Figure 4.

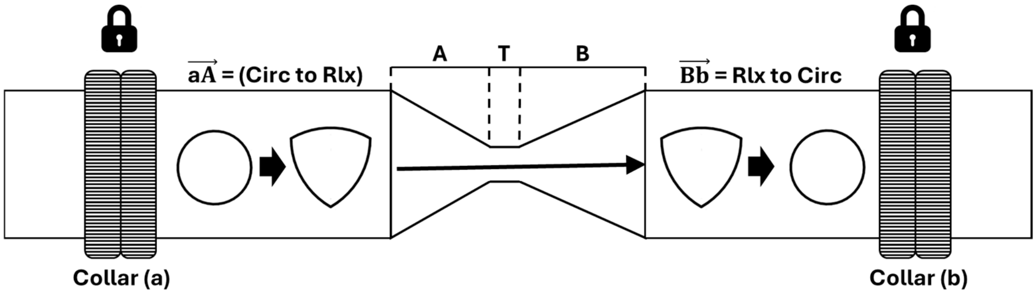

Figure 4. In-line integration of the DVRA module within a Venturi duct. Segment $\overrightarrow{aA}$ provides the internal cross-section transition from circular to a Reuleaux profile, whereas segment $\overrightarrow{Bb}$ provides the reverse transition from Reuleaux to circular. Both segments are directional and must be installed according to the orientation indicated by the upper arrow. Collars a and b allow the module to rotate; the closed padlocks indicate the collars are locked in place. The arrow along the Venturi denotes the flow direction. A: converging section; T: throat; B: diverging section.

4. Dynamic Throat Regulation

DVRA throat regulation is achieved by acting on the local section in the vicinity of the constriction, thereby modifying the conditions that govern cavitation inception and the stability of the cavitating regime [7–10]. In this work, the throat is not treated as a fixed geometry but as a configuration variable that can be modulated over time through actuation, while the structural reference associated with the throat remains stable and is used as a frame for definitions and control [17–21]. The elastomeric surface enables controlled and continuous deformation, avoiding internal wall discontinuities and making regulation compatible with in-line operation. The dynamic-throat concept is illustrated in Figure 5.

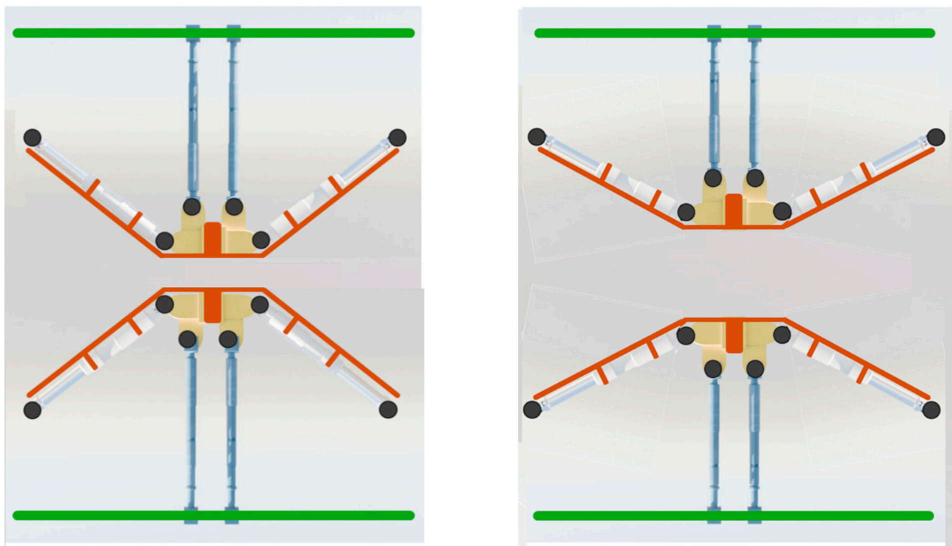

(**a**) (**b**)

Figure 5. Dynamic-throat concept in the DVRA. Panel (**a**) shows the minimum achievable equivalent diameter, while panel (**b**) shows the maximum achievable equivalent diameter, as governed by the elastomer properties and actuator stroke. The reference throat is highlighted in yellow, whereas the effective hydraulic throat is defined by the elastomeric liner in red. The actuation system (blue) deforms the liner, thereby modifying the throat cross-section at T; the green bars indicate the external fixed support and the anchoring constraints for the actuators. Color code: reference throat (yellow), structural cage (white), elastomeric liner/hydraulic surface (red), liner actuators (blue), external fixed support/anchoring constraint (green), and 360° spherical joints (black).

Variation in the hydraulic throat is specified by normalized inputs $u_i(t) \in [0,1]$, collected in the vector $\mathbf{u}(t)$. This section considers only the throat component $\mathbf{u}_g(t) = [u_1(t), \ldots, u_N(t)]^T$, which governs liner deformation. No specific constitutive law is assumed for the liner; instead, the existence of a repeatable relationship between $\mathbf{u}_g(t)$ and the resulting hydraulic geometry is assumed, defined within a declared operating domain. The throat is described operationally through equivalent quantities such as the area $A_T(\mathbf{u}_g)$ and, when useful, the wetted perimeter $P_T(\mathbf{u}_g)$ and the equivalent hydraulic diameter $d_{eq}(\mathbf{u}_g) = 4A_T(\mathbf{u}_g)/P_T(\mathbf{u}_g)$.

The elastomeric liner may introduce non-idealities, including hysteresis and dependencies on temperature and loading conditions, which are treated as part of the operating domain. For implementation and replicability, it is therefore necessary to specify the achievable throat range and the constraints imposed by kinematics and actuation, together with the repeatability requirements of the command–geometry relationship. To this end, it is useful to report the minimum parameters that characterize throat regulation, including the maximum command excursion of $u_i(t)$, the corresponding excursion of the throat geometric quantities, and the characteristic axial length of the throat region along the module axis [25].

In this formulation, $\mathbf{u}_g(t)$ constitutes the command, and the effective hydraulic throat constitutes the configurational variable that modifies the local flow conditions and, indirectly, the cavitation operating window. Throat regulation remains available regardless of whether the A-T-B element is in the free or locked state, because it acts on the liner geometry and does not require relative rotations between segments.

5. Swirl Forcing and DVRA-CR and DVRA-RR Operating Modes

Swirl forcing is the second configurational action of the DVRA and enables a rotational boundary condition to be imposed at the device ends without rotating elements immersed in the fluid [26,27]. In this work, swirl is defined in an operational sense and does not require quantification of the tangential flow field in the fluid, which would require dedicated measurements or simulations.

The forcing is implemented through external collars at ends A and B that impose the angular velocities $\omega_A(t)$ and $\omega_B(t)$. Rotation is transferred to the mechanical cage and the elastomeric liner, whereas the process line does not rotate. The device includes an A-T-B element with 360° spherical joints and can operate in a locked or free state. Swirl forcing requires the free state, and in the DVRA-RR mode the reference at T is additionally constrained to make the direction reversal across the throat unambiguous.

Operating modes are defined with respect to section T, which separates the A-T and T-B segments. The baseline mode corresponds to $\omega_A = \omega_B = 0$. The DVRA-CR mode, where CR denotes concordant rotation, describes configurations in which the forcing direction is consistent upstream and downstream of the throat, whereas the DVRA-RR mode, where RR denotes reversed rotation, describes configurations in which the forcing direction reverses across section T. The classification as a function of the A-T-B state and the state of reference at T is reported in Table 1.

To fix the flow-direction convention and the locked/free constraint notation used in the operating modes, the conceptual configuration scheme is reported in Figure 6.

The flow direction is assumed from left to right. Padlock symbols indicate the rotation-constraint state, with a closed padlock denoting the locked state and an open padlock denoting the free state. Arrows qualitatively indicate the direction of the tangential forcing in the A-T and T-B segments. In the DVRA-CR mode, the forcing does not reverse across T. In the DVRA-RR mode, the forcing reverses across T and section T must be locked to make the distinction between the two segments unambiguous. An overall view of the DVRA and a visualization of the module interior are reported in Figure 7.

Table 1. DVRA operating modes defined with respect to the throat section T.

Item	Baseline	DVRA-CR	DVRA-RR
Swirl-forcing	no	yes	yes
Rotating collar A	OFF $\Rightarrow \omega_A(t) = 0$	ON $\Rightarrow \omega_A(t) \neq 0$	ON $\Rightarrow \omega_A(t) \neq 0$
Rotating collar B	OFF $\Rightarrow \omega_B(t) = 0$	ON $\Rightarrow \omega_B(t) \neq 0$	ON $\Rightarrow \omega_B(t) \neq 0$
A-T-B element	locked	free	free
Throat reference T	locked	free or locked	locked
Rel. Dir. A $\to$ T	-	$\uparrow$	$\uparrow$
Rel. Dir. T $\to$ B	-	$\uparrow$	$\downarrow$
Criterion	$\omega_A(t) = 0, \omega_B(t) = 0$	$\Omega_{AT}(t) \cdot \Omega_{TB}(t) \geq 0$	$\Omega_{AT}(t) \cdot \Omega_{TB}(t) < 0$

Note: Swirl-forcing indicates rotational boundary conditions imposed at the module ends. The end wheels/collars at A and B impose the angular velocities $\omega_A(t)$ and $\omega_B(t)$. Relative rotations with respect to the throat section T are defined as $\Omega_{AT}(t) = \omega_A(t) - \omega_T(t)$ and $\Omega_{TB}(t) = \omega_T(t) - \omega_B(t)$. Arrows qualitatively indicate the sign of Ω_{AT} and Ω_{TB}, while "-" denotes no imposed forcing. The baseline mode corresponds to $\omega_A(t) = 0$ and $\omega_B(t) = 0$, and mode classification follows the sign of $\Omega_{AT}(t) \cdot \Omega_{TB}(t)$ ($\geq$0 for DVRA-CR, <0 for DVRA-RR). When T is free, ω_T is not imposed; therefore, Ω_{AT} and Ω_{TB} can be evaluated only if ω_T is measured or estimated, whereas for DVRA-RR the reference at T is locked by definition, making $\omega_T = 0$ and the classification unambiguous.

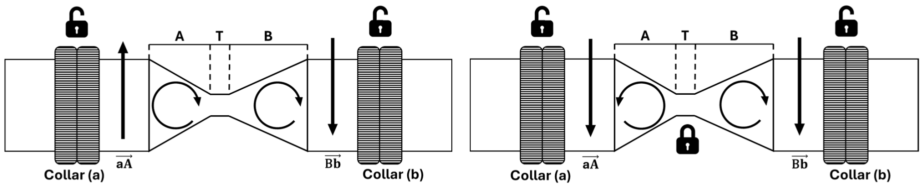

(**a**) (**b**)

Figure 6. Conceptual schemes of DVRA operating modes with respect to the throat section T. Panel (**a**) DVRA-CR: opposite collar actuation (left ↑, right ↓) determines a co-rotating condition (↻↻) on both sides of the throat T. Panel (**b**) DVRA-RR: with the throat T locked, same-direction collar actuation (both ↓) determines reverse rotation (↺↻) between the upstream and downstream sides of T. The directional segments $\vec{aA}$ and $\vec{Bb}$ are actuated by collar (a) and collar (b); open padlocks indicate the collar is unlocked, i.e., adjustable. The vertical arrows (↑ / ↓) denote the actuation direction imposed by the collar on the segments, whereas the ↺ / ↻ symbols indicate the resulting sense of rotation of the internal profile in the converging section A and diverging section B. Open/closed padlocks indicate the collars in the unlocked/locked state, respectively.

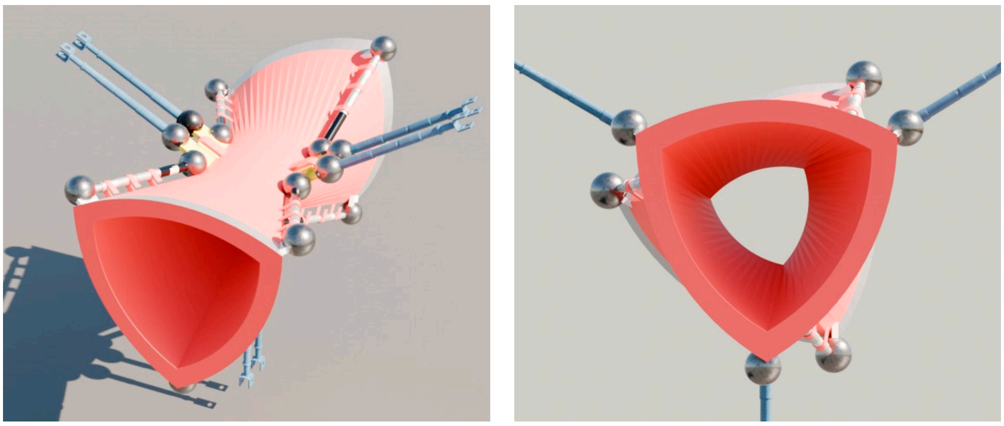

(**a**) (**b**)

Figure 7. DVRA module after enabling boundary-imposed swirl forcing, relative to the baseline configuration. (**a**) Overall view of the module. (**b**) Front view showing the internal subsystem made of the mechanical cage and the elastomeric liner rotated with respect to the external reference as a result of the rotation imposed at the module ends. These modes define a finite set of operating configurations that can be used as configuration selectors. Mode selection can be combined with throat regulation to manage the in-line cavitation regime. Color code: reference throat (yellow), structural cage (white), elastomeric liner/hydraulic surface (red), liner actuators (blue), and 360° spherical joints (black).

6. Admissible Inputs and Design Space of the DVRA

To describe the DVRA in an unambiguous and reproducible manner, an admissible input set $\mathcal{U}$, defined over dimensionless commands, and a design space $\mathcal{D}$, defined over the configuration vector $\mathbf{x}$, are introduced. The configuration includes the effective hydraulic-throat geometry at section T and the boundary-imposed swirl forcing at sections A and B. The kinematics of the A-T-B element, expressed by the free or locked state, is treated as a mode parameter and is recalled in the definition of the operating modes.

The vector of dimensionless inputs $\mathbf{u}(t)$ is defined in (1), where $u_1(t), \ldots, u_N(t)$ command liner reconfiguration and $u_A(t)$ and $u_B(t)$ command boundary-imposed swirl forcing. The admissible input set is defined as

$$\mathcal{U} = \left\{ \mathbf{u} \;\middle|\; \begin{array}{c} u_i \in [0,\ 1], \quad i = 1, \ldots,\ N \\ u_A \in [0,\ 1], \\ u_B \in [0,\ 1] \end{array} \right\} \tag{4}$$

In the following, $\mathbf{u}(t) \in \mathcal{U}$ is assumed. The parameter N depends on the mechanical implementation and on the actuation discretization.

The boundary-imposed angular velocities are obtained by scaling within the admissible limits:

$$\omega_A(u_A) = \omega_A^{min} + u_A\left(\omega_A^{max} - \omega_A^{min}\right) \tag{5}$$

The same definition is adopted for the outlet boundary:

$$\omega_B(u_B) = \omega_B^{min} + u_B\left(\omega_B^{max} - \omega_B^{min}\right) \tag{6}$$

The normalized commands $u_A, u_B \in [0,\ 1]$ are unsigned. The direction of the imposed boundary rotation is therefore encoded in the admissible limits $(\omega_{A,min}, \omega_{A,max})$ and $(\omega_{B,min}, \omega_{B,max})$. In particular, if the limits straddle zero (e.g., $\omega_{A,min} < 0 < \omega_{A,max}$), then the sign of ω_A can change even though u_A is unsigned. The neutral command associated with $\omega_A = 0$ is $u_{A,0} = -\omega_{A,min}/(\omega_{A,max} - \omega_{A,min})$ (analogously for B). In industrial implementations, the same mapping can be realized equivalently as a magnitude command in [0, 1] plus a direction bit.

The throat-input subvector is denoted by $\mathbf{u}_g(t) = \left[u_1(t), \ldots, u_N(t)\right]^T$. The effective hydraulic throat at section T is described by the area $A_T(\mathbf{u}_g)$ and the wetted perimeter $P_T(\mathbf{u}_g)$ of the internal section effectively seen by the fluid. The equivalent hydraulic diameter is introduced as

$$d_{eq}(\mathbf{u}_g) = \frac{4\ A_T(\mathbf{u}_g)}{P_T(\mathbf{u}_g)} \tag{7}$$

This definition is also valid for non-circular sections, including a Reuleaux-triangle throat. The throat region is further described through equivalent parameters $L_t(\mathbf{u}_g)$, $\alpha_{in}(\mathbf{u}_g)$, and $\alpha_{out}(\mathbf{u}_g)$, where L_t is the equivalent length of the throat region and α_{in} and α_{out} are the equivalent angles of the converging and diverging sections. The mappings $A_T(\cdot)$, $P_T(\cdot)$, $L_t(\cdot)$, $\alpha_{in}(\cdot)$, and $\alpha_{out}(\cdot)$ are determined by the liner kinematics and can be obtained through a geometric–kinematic mapping or calibration.

A compact configuration vector is then defined as:

$$\boldsymbol{x}(\mathbf{u}) = \begin{bmatrix} d_{eq}(\mathbf{u}_g) \\ L_t(\mathbf{u}_g) \\ \alpha_{in}(\mathbf{u}_g) \\ \alpha_{out}(\mathbf{u}_g) \\ \omega_A(\mathbf{u}_A) \\ \omega_B(\mathbf{u}_B) \end{bmatrix} \tag{8}$$

The design space $\mathcal{D}$ is the set of admissible configurations:

$$\mathcal{D} = \{\mathbf{x}\,|\mathbf{x} = \mathbf{x}(\mathbf{u}), \quad \mathbf{u} \in \mathcal{U}\} \tag{9}$$

Although the present implementation uses a Reuleaux triangular throat, the design space $\mathcal{D}$ is defined through normalized inputs and equivalent hydraulic descriptors of the throat section, including cross-sectional area, wetted perimeter, and hydraulic diameter. These descriptors are well-defined for arbitrary cross-sectional shapes, so the framework is not restricted to the Reuleaux geometry. Extending the framework to a different throat shape only requires updating the geometric–kinematic mapping that relates actuator commands to the equivalent descriptors, together with the corresponding admissible bounds. Scaling to different pipeline sizes follows the same normalized formulation, with geometric variables expressed relative to the line diameter and the admissible set re-identified from actuator stroke limits, liner characteristics, and collar speed limits.

Equivalently, $\mathcal{D}$ can be described through operational limits related to geometry, materials, and actuation:

$$\mathcal{D} = \left\{ x \,\middle|\, \begin{array}{c} d_{eq}^{min} \le d_{eq} \le d_{eq}^{max} \\ L_t^{min} \le L_t(u_g) \le L_t^{max} \\ \alpha_{in}^{min} \le \alpha_{in} \le \alpha_{in}^{max} \\ \alpha_{out}^{min} \le \alpha_{out} \le \alpha_{out}^{max} \\ \omega_A^{min} \le \omega_A \le \omega_A^{max} \\ \omega_B^{min} \le \omega_B \le \omega_B^{max} \end{array} \right\} \tag{10}$$

Kinematic constraints and non-idealities further restrict the configurations that are practically achievable. Therefore, an achievable subset of inputs $\mathcal{U}_R \subseteq \mathcal{U}$ is introduced, together with the corresponding set of achievable configurations:

$$\mathcal{D}_R = \{\mathbf{x}\,|\mathbf{x} = \mathbf{x}(\mathbf{u}), \quad \mathbf{u} \in \mathcal{U}_R\} \tag{11}$$

Operating modes are defined with respect to the throat section T, which separates the upstream segment A-T from the downstream segment T-B. The baseline mode is defined by the absence of boundary-imposed swirl. The DVRA-CR mode corresponds to a tangential forcing that is concordant upstream and downstream of the throat and can be implemented with the reference at T either free or locked. The DVRA-RR mode corresponds to a tangential forcing that is discordant across T and requires the reference at T to be locked.

When the reference at T is constrained, $\omega_T = 0$ is assumed; therefore, $\Omega_{AT} = \omega_A$ and $\Omega_{TB} = -\omega_B$. The operating mode is determined by the sign of $\Omega_{AT} \cdot \Omega_{TB}$ (Table 1), as illustrated in Table 2.

Table 2. Minimal example of baseline/DVRA-CR/DVRA-RR classification (case $\omega_T = 0$).

Item	Baseline	DVRA-CR	DVRA-RR
ω_A	0	+	+
ω_B	0	-	+
$\Omega_{AT} \cdot \Omega_{TB}$	0	> 0	< 0

Note: "+" and "-" denote the sign of the boundary-imposed angular velocities ω_A and ω_B after scaling Equations (5) and (6). Although $u_A, u_B \in [0, 1]$ are unsigned, sign changes are permitted whenever the admissible limits straddle zero (e.g., $\omega_{A,min} < 0 < \omega_{A,max}$ and/or $\omega_{B,min} < 0 < \omega_{B,max}$); otherwise, the sign is fixed by the chosen limits. For implementation, the same mapping can be realized as a magnitude command in [0, 1] plus a direction bit.

The proposed formulation is grounded in how throat configuration and boundary-imposed swirl act on the pressure field governing cavitation. For a given flow rate, the throat setting determines the mean throat velocity $V_T = Q/A_T$ and thus the characteristic dynamic-pressure scale. Cavitation propensity depends on the local minimum pressure relative to vapor pressure and may be characterized by a cavitation index based on the available pressure level and V_T. Boundary-imposed swirl alters the pressure field through a radial pressure gradient and axial-momentum redistribution, which can shift both the location and value of the minimum pressure in the throat and diffuser region. Throat configuration and boundary-imposed swirl therefore act on the same governing quantity, the minimum pressure, and their effects are expected to be coupled with respect to cavitation onset and extent. Table 3 summarizes representative Baseline, DVRA-CR, and DVRA-RR cases and the associated throat-velocity scaling.

Table 3. Representative command-level instantiation of Baseline, DVRA-CR, and DVRA-RR boundary-imposed modes.

Item	Baseline	DVRA-CR	DVRA-RR
Boundary inputs	$u_A = u_{A,0},\ u_B = u_{B,0}$	choose u_A, u_B such that $\omega_A(u_A) > 0,\ \omega_B(u_B) < 0$	choose u_A, u_B such that $\omega_A(u_A) > 0,\ \omega_B(u_B) > 0$
Boundary angular velocities	$\omega_A = 0,\ \omega_B = 0$	$\omega_A > 0,\ \omega_B < 0$	$\omega_A > 0,\ \omega_B > 0$
Mode criterion	$\omega_A = 0,\ \omega_B = 0$	$\Omega_{AT} \cdot \Omega_{TB} \geq 0$	$\Omega_{AT} \cdot \Omega_{TB} < 0$

Note: In all modes, the throat setting is commanded by u_g and determines the throat area $A_T(u_g)$, hence the throat-velocity scale $V_T = Q/A_T$. $u_{A,0}$ and $u_{B,0}$ denote the neutral commands yielding $\omega_A = 0$ and $\omega_B = 0$, as defined after Equations (5) and (6). $\omega_A(u_A)$ and $\omega_B(u_B)$ follow Equations (5) and (6). Ω_{AT} and Ω_{TB} are defined in Equations (2) and (3), and mode labels follow Table 1 with the sign convention illustrated in Table 2. This table provides a reproducible instantiation of the framework variables and does not constitute validation of the generated swirl field or cavitation performance.

7. Control-Oriented Framework and Inverse Mapping

The DVRA is an in-line actuatable module that enables regulation of the cavitating regime through device configuration. In continuous processes, the operational objective is to keep cavitation within a target band despite variations in flow rate, available pressure, temperature, and fluid properties. A control-oriented framework links in-line measurements to configuration variables and actuator commands.

Regulation is achieved through two configurational actions. The first concerns the effective hydraulic throat at section T, modulated by the commands $u_i(t)$. The second concerns boundary-imposed swirl forcing, specified by $u_A(t)$ and $u_B(t)$, which imposes rotational boundary conditions and enables the baseline, DVRA-CR, and DVRA-RR operating modes. In this work, these actions are treated as configuration variables, and the availability of measured or simulated fluid-dynamic fields is not assumed.

The problem is formulated as the selection of an achievable configuration $\mathbf{x} \in \mathcal{D}_R$ from inputs $\mathbf{u}(t) \in \mathcal{U}$. The formulation is inverse in nature: given a target band for a cavitation indicator that can be estimated in line, such as the cavitation number or an equivalent metric, the regulation selects $\mathbf{u}(t)$ and the operating mode to keep the indicator within the band. Performance under disturbances and process variations depends on application-specific characterization.

Implementation requires a sensor–actuator loop based on industrial measurements. Figure 8 reports a conceptual diagram in which flow rate, pressure, and temperature feed the estimation of the cavitation indicator; comparison with the target generates configuration commands, which are translated into $u_i(t)$, $u_A(t)$, and $u_B(t)$.

https://doi.org/10.3390/jmmp10030081

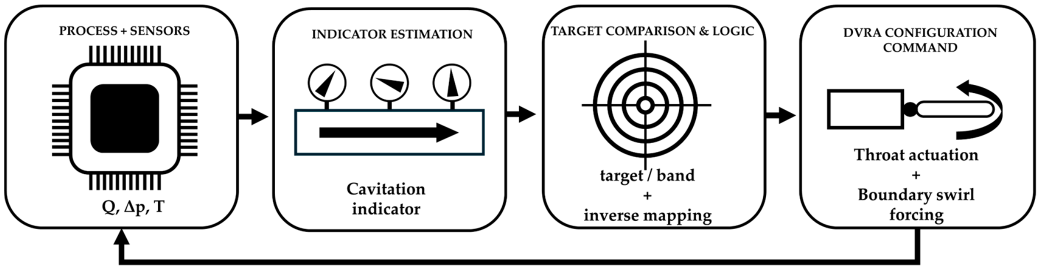

Figure 8. Conceptual block diagram for in-line regulation using the DVRA. Process measurements feed an estimate of a cavitation indicator; comparison with a target/band generates configuration commands acting on the throat geometry and on the boundary-imposed swirl. Arrows indicate signal flow; the bottom arrow denotes closed-loop feedback from the DVRA command to the process. Measured variables are Q (flow rate), Δp (pressure drop), and T (temperature).

8. Implementability, Replicability, and Scope Limitations

The DVRA is designed for installation as an in-line module. The architecture separates the process line from the actuation subsystem by confining throat regulation and boundary-imposed swirl forcing within the device through the mechanical cage, the elastomeric liner, and the end collars at sections A and B. The process line does not need to rotate, thereby reducing plant impact and simplifying integration in continuous processes.

Replicability requires reporting the geometric references and the DVRA degrees of actuation. The minimum information required to reconstruct the module geometry, to describe the effective hydraulic throat at section T, and to reproduce the logic of the operating modes defined with respect to T should be provided. This minimum information is summarized in Table 4.

Table 4. Key information to report for DVRA replicability.

Item	Content	Purpose
Geometry	Venturi dims; Reuleaux section; round↔Reuleaux transitions	Rebuild module
Throat	Reference vs. effective throat in T; achievable range A_T/d_{eq}; liner material family/continuity	Controlled variable
Actuation & kinematics	Actuator count/layout; command range u_i; stroke limits; cage; 360° joints; A − T − B locked/free	Implementability
Swirl	End collars at A and B; ω_A, ω_B limits; command logic	Imposed swirl
Modes	baseline/CR/RR definition vs. T	Operational ID

The elastomeric liner enables a variable throat and a continuous internal surface, but it introduces non-idealities that should be reported. The response to the commands $u_i(t)$ may exhibit hysteresis and dependencies on temperature and loading conditions. In industrial operation, these effects can be mitigated through feedback control, provided that the command–geometry relationship is repeatable within a defined operating domain and after calibration or identification.

Swirl forcing may also introduce non-idealities. Torque transmission to the collars may lead to backlash, dead zones, and saturation, which are considered part of the operating domain. Moreover, the spherical joints improve kinematic compatibility but impose finite limits on admissible angles and loads. The combination of boundary-imposed torsion and throat reconfiguration should therefore remain within a configurational envelope that avoids interference, actuator saturation, and excessive liner stresses.

This work focuses on device architecture, operational definitions, and a control-oriented framework. Neither CFD nor dedicated experimental campaigns are employed, because cavitation predictions without data and without verification and validation would not be sufficiently robust [28–33]. Moreover, transient cavitation CFD is strongly fluid-specific and depends on cavitation-model calibration, so a single-fluid numerical case would have limited generality relative to the scope of the present framework. The DVRA-CR and DVRA-RR modes are defined at the configurational level as boundary-imposed operating conditions. The present manuscript focuses on these configurational definitions; quantitative swirl-field characterization and cavitating-regime assessment under application-specific conditions require dedicated measurements or simulations and are not addressed here. At this stage, the objective is to provide an implementable basis to treat in-line cavitation as a variable that can be regulated through device configuration.

9. Conclusions

This work presents the DVRA as an in-line actuatable Venturi module and a control-oriented framework for configuration-based cavitation regulation in continuous processes. The main contributions are:

- A clear operational distinction is introduced between the reference throat (structural/geometric reference) and the effective hydraulic throat seen by the fluid, described through equivalent descriptors including A_T, P_T, and d_{eq}.
- Boundary-imposed swirl forcing is formalized through $\omega_A(t)$, $\omega_B(t)$ and the relative rotations $\Omega_{AT}(t)$, $\Omega_{TB}(t)$, enabling an unambiguous classification of Baseline, DVRA-CR, and DVRA-RR operating modes with respect to the throat section T.
- A normalized admissible input set $\mathcal{U}$ and a configuration-space formulation $\mathcal{D}$, together with an achievable subset $\mathcal{D}_R$, are introduced to distinguish admissible from practically achievable configurations for reproducible implementation.
- Regulation is cast as an inverse-mapping problem: given a target band for an in-line estimated cavitation indicator and standard industrial measurements of flow rate, pressure, and temperature, configuration commands are selected to keep the indicator within bounds.
- A physical rationale is provided for the expected coupling between throat configuration and boundary-imposed swirl through their joint action on the minimum-pressure field governing cavitation; the contribution is methodological and intended as an implementable basis for subsequent application-specific characterization and as a set of reproducible framework outcomes.

Funding: This research received no external funding.

Institutional Review Board Statement: Not applicable.

Informed Consent Statement: Not applicable.

Data Availability Statement: The original contributions presented in this study are included in the article. Further inquiries can be directed to the corresponding author.

Conflicts of Interest: The author declares no conflicts of interest.

Abbreviations

The following abbreviations are used in this manuscript:

DVRA	Dynamic Venturi Reuleaux Actuated
DVRA-CR	Dynamic Venturi Reuleaux Actuated (Co-Rotating)
DVRA-RR	Dynamic Venturi Reuleaux Actuated (Reverse Rotation)

References

1. Pandit, A.B.; Gogate, P.R. A review and assessment of hydrodynamic cavitation as a technology for the future. *Ultrason. Sonochem.* **2005**, *12*, 21–27. [CrossRef]
2. Carpenter, J.; Badve, M.; Rajoriya, S.; Pandit, A.B. Hydrodynamic cavitation: An emerging technology for the intensification of various chemical and physical processes in a chemical process industry. *Rev. Chem. Eng.* **2017**, *33*, 433–468. [CrossRef]
3. Zheng, H.; Zheng, Y.; Zhu, J. Recent developments in hydrodynamic cavitation reactors: Cavitation mechanism, reactor design, and applications. *Engineering* **2022**, *19*, 180–198. [CrossRef]
4. Galloni, M.G.; Fabbrizio, V.; Giannantonio, R.; Falletta, E.; Bianchi, C.L. Applications and applicability of the cavitation technology. *Curr. Opin. Chem. Eng.* **2025**, *48*, 101129. [CrossRef]
5. Malkapuram, S.T.; Sonawane, S.H. Intensified physical and chemical processing using cavitation: How far are we from commercial applications of hydrodynamic cavitation? *Curr. Opin. Chem. Eng.* **2025**, *49*, 101154. [CrossRef]
6. Manoharan, D.; Zhao, J.; Ranade, V.V. Cavitation technologies for extraction of high value ingredients from renewable biomass. *TrAC Trends Anal. Chem.* **2024**, *174*, 117682. [CrossRef]
7. Brennen, C.E. *Cavitation and Bubble Dynamics*; Oxford University Press: Oxford, UK, 1995. [CrossRef]
8. Franc, J.-P.; Michel, J.-M. *Fundamentals of Cavitation*; Kluwer Academic Publishers: Dordrecht, The Netherlands, 2004. [CrossRef]
9. Groß, T.F.; Pelz, P.F. Diffusion-driven nucleation from surface nuclei in hydrodynamic cavitation. *J. Fluid Mech.* **2017**, *830*, 138–164. [CrossRef]
10. Panda, D.; Saharan, V.K.; Manickam, S. Controlled hydrodynamic cavitation: A review of recent advances and perspectives for greener processing. *Processes* **2020**, *8*, 220. [CrossRef]
11. Bashir, T.A.; Soni, A.G.; Mahulkar, A.V.; Pandit, A.B. The CFD driven optimization of a modified Venturi for cavitation activity. *Can. J. Chem. Eng.* **2011**, *89*, 1366–1375. [CrossRef]
12. Li, M.; Bussonnière, A.; Bronson, M.; Xu, Z.; Liu, Q. Study of Venturi tube geometry on the hydrodynamic cavitation for the generation of microbubbles. *Miner. Eng.* **2019**, *132*, 268–274. [CrossRef]
13. Nadiri, K.; Baradaran, S. Geometric optimization of Venturi reactors for enhanced hydrodynamic cavitation efficiency: From conventional to advanced tandem configurations. *Chem. Eng. J. Adv.* **2025**, *24*, 100844. [CrossRef]
14. Simpson, A.; Ranade, V.V. Modeling hydrodynamic cavitation in Venturi: Influence of Venturi configuration on inception and extent of cavitation. *AIChE J.* **2019**, *65*, 421–433. [CrossRef]
15. Wang, G.; Senocak, I.; Shyy, W.; Ikohagi, T.; Cao, S. Dynamics of attached turbulent cavitating flows. *Prog. Aerosp. Sci.* **2001**, *37*, 551–581. [CrossRef]
16. Podbevšek, D.; Petkovšek, M.; Ohl, C.D.; Dular, M. Kelvin–Helmholtz instability governs the cavitation cloud shedding in Venturi microchannel. *Int. J. Multiph. Flow* **2021**, *142*, 103700. [CrossRef]
17. Viswanathan, S. Development of a pressure drop model for a variable throat Venturi scrubber. *Chem. Eng. J.* **1998**, *71*, 153–160. [CrossRef]
18. Brady, J.D.; Legatski, L.K. Variable Throat Venturi Scrubber. U.S. Patent US4,023,942A, 17 May 1977.
19. Tian, H.; Zeng, P.; Yu, N.; Cai, G. Application of variable area cavitating Venturi as a dynamic flow controller. *Flow Meas. Instrum.* **2014**, *38*, 21–26. [CrossRef]
20. Tan, G.; Tian, H.; Gu, X.; Meng, X.; Wei, T.; Zhang, Y.; Cai, G. Flow feedback control based on variable area cavitating Venturi and its application in hybrid rocket motors. *Acta Astronaut.* **2023**, *211*, 238–248. [CrossRef]
21. Long, X.; Sun, M.; Chen, L.; Li, Q.; Cheng, P. Research on cavitation and oscillation transition mechanism of adjustable cavitation Venturi tube. *J. Hydrodyn.* **2025**, *37*, 680–697. [CrossRef]
22. Havil, J. Chapter Seven. Curves of Constant Width. In *Curves for the Mathematically Curious: An Anthology of the Unpredictable, Historical, Beautiful, and Romantic*; Princeton University Press: Princeton, NJ, USA, 2019; pp. 104–125. [CrossRef]
23. Albanese, L. The Venturi Reuleaux Triangle: Advancing sustainable process intensification through controlled hydrodynamic cavitation in food, water, and industrial applications. *Sustainability* **2025**, *17*, 6812. [CrossRef]
24. Albanese, L.; Centritto, M.; Meneguzzo, F. Apparatus for Dynamically Regulating Hydrodynamic Cavitation Processes and Related Process. European Patent EP4260934A1, 18 October 2023.
25. *ISO 37:2017*; Rubber, Vulcanized or Thermoplastic—Determination of Tensile Stress–Strain Properties. International Organization for Standardization: Geneva, Switzerland, 2017.
26. Petkovšek, M.; Zupanc, M.; Dular, M.; Kosjek, T.; Heath, E.; Kompare, B.; Širok, B. Rotation generator of hydrodynamic cavitation for water treatment. *Sep. Purif. Technol.* **2013**, *118*, 415–423. [CrossRef]
27. Wang, J.; Guo, Y.; Guo, P.; Yu, J.; Guo, W.; Wang, X. Degradation of reactive brilliant red K-2BP in water using a combination of swirling jet-induced cavitation and Fenton process. *Sep. Purif. Technol.* **2014**, *130*, 1–6. [CrossRef]
28. Charrière, B.; Decaix, J.; Goncalvès, E. A comparative study of cavitation models in a Venturi flow. *Eur. J. Mech. B Fluids* **2015**, *49*, 287–297. [CrossRef]

29. Geng, L.; Escaler, X. Assessment of RANS turbulence models and Zwart cavitation model empirical coefficients for the simulation of unsteady cloud cavitation. *Eng. Appl. Comput. Fluid Mech.* **2020**, *14*, 151–167. [CrossRef]
30. Chebli, R.; Audebert, B.; Zhang, G.; Coutier-Delgosha, O. Influence of the turbulence modeling on the simulation of unsteady cavitating flows. *Comput. Fluids* **2021**, *221*, 104898. [CrossRef]
31. De la Cruz-Ávila, M.; De León-Ruiz, J.E.; Carvajal-Mariscal, I.; Klapp, J. CFD turbulence models assessment for the cavitation phenomenon in a rectangular profile Venturi tube. *Fluids* **2024**, *9*, 71. [CrossRef]
32. Rütten, E.; Leister, N.; Karbstein, H.P.; Håkansson, A. Possibilities and limits of modeling cavitation in high-pressure homogenizers—A validation study. *Chem. Eng. Sci.* **2024**, *283*, 119405. [CrossRef]
33. Zeman, R.; Rudolf, P. Optimizing Venturi nozzle design for enhanced cavitation and pressure dynamics: A comparative analysis of turbulence models for cavitating flow characterization. *Eng. Mech.* **2024**, *30*, 326–329. [CrossRef]